A Seasonally Varying Phenology for High Resolution Simulations with the COSMO-CLM Model

Eva Nowatzki[1],
Jan-Peter Schulz[2],
Jean-Marie Bettems[3],
Jürg Luterbacher[1,4],
Merja Tölle[1]

[1] Department of Geography, Climatology, Climate Dynamics and Climate Change, Justus-Liebig University Giessen, Giessen, Germany
[2] Deutscher Wetterdienst (DWD, German Meteorological Service), Offenbach, Germany
[3] MeteoSwiss, Zurich, Switzerland
[4] World Meteorological Organization (WMO), Science and Innovation Department, Geneva, Switzerland

Motivation

- Phenology and its interannual variability are altered through anthropogenic climate change (Parmesan and Yohe 2003; Settele et al. 2014)
  - Growing season in temperate Europe lengthened already and will further with warmer conditions (Menzel and Fabian 1999; Reyes-Fox et al. 2014)
- Phenology influences the energy and water cycle of the regional climate as well as other variables through albedo, sensible and latent heat flux changes (Peñuelas and Filella 2009)
- Phenology depends on the vegetation type, temperature, precipitation and day length (White et al. 1997; Oleksyn et al. 1992)
- Sophisticated land surface models have high computational costs and a rather coarse horizontal resolution
- The phenology of the regional climate model COSMO-CLM (CCLM) with land surface TERRA-ML is static and independent of the environment

Summary and Outlook

- Comparing the newly implemented phenology with the standard phenology of CCLM it shows a significantly higher correlation to observations
- The interannual variability of leaf area index (LAI), notably the extreme years, also improved
- The start of the growing season interannually varies with winter and spring temperature
- Extreme warm days and heavy precipitation events are influenced by phenology and can be improved with the new module
- Reduced LAI in dry summers lead to lower latent heat flux

→ Human impact on vegetation (e.g. harvesting) needs a specific approach

→ More vegetation types have to be studied and implemented

→ Simulations are needed over a larger domain

Menzel, Annette, and Peter Fabian. *Nature* (1999): https://doi.org/10.1038/17709
Oleksyn, Jacek, Mark G. Tjoelker, and Peter B. Reich. *New Phytologist* (1992): https://doi.org/10.1111/j.1469-8137.1992.tb01806.x
Parmesan, Camille, and Gary Yohe. *Nature* (2003): https://doi.org/10.1038/nature01286
Peñuelas, Josep, and Iolanda Filella. *Science* (2009): https://doi.org/10.1126/science.1173004
Reyes-Fox, Melissa, et al. *Nature* (2014): https://doi.org/10.1038/nature13207
Settele, J., et al. IPCC (2014): https://doi.org/10.1017/CBO9781107415379.009
White, Michael A., Peter E. Thornton, and Steven W. Running. *Global biogeochemical cycles* (1997): https://doi.org/10.1029/97GB00330

The Experiment

Data

- Lindenberg: Meteorological Observatory (temperature and precipitation)
- Linden: GiFACE project (Jager et al. 2003; Andresen et al. 2018) (temperature and precipitation)
- Selhausen: TERENO project (Post et al. 2018; Bogena et al. 2018) (temperature); DWD station Jülich (precipitation)
- HYRAS gridded data set (1 km, daily) (Rauthe et al. 2013) (daily maximum temperature and daily precipitation sum)
- LAI: gridded satellite product of SPOT and PROBA-V (1 km, 10 days) (Baret et al. 2013; Camacho et al. 2013)

Model

- COSMO-CLM-v5.0_clm15
- INT2LM-v2.05_clm1
- ERA-Interim forced
- External data modified to grass
- two time-level Runge-Kutta
- model time step 25 seconds
- shallow convection Tiedtke
- Land-surface TERRA-ML
- 0.0275° (3 km)
- 3 single columns
- 1999-2015

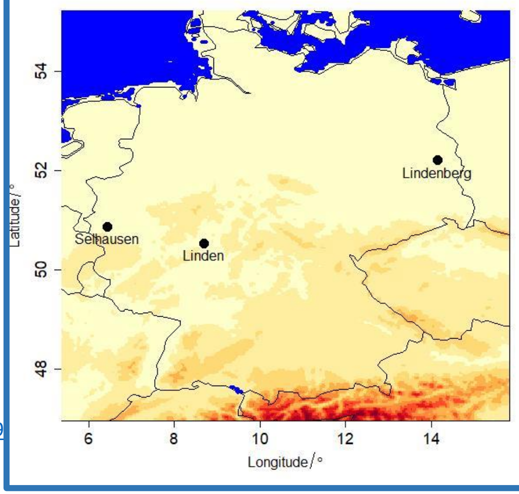

Methods

1. Standard: Annually recurring leaf area index (LAI) calculated in INT2LM, depending on latitude and altitude (**_old**)
2. Newly implemented calculation of LAI depending on surface temperature (Knorr et al. 2010; Schulz et al. 2015) (**_T**)
   → growing starts when the surface temperature (weighted over a past period) exceeds a threshold value (5°C) and ends when the temperature is below
3. The same as in 2 + dependence on day length (**_TD**)
   → growing starts when the surface temperature (weighted over a past period) and the day length exceed threshold values (5°C, 10h) and ends when they are below
4. The same as in 3 + dependence on water availability (**_TDW**)
   → growing starts when the surface temperature (weighted over a past period) and the day length exceed threshold values (5°C, 10h) and ends when they are below + reduction of LAI according to the water available in the related soil

Andresen, Louise C., et al. *Global Change Biology* (2018): https://doi.org/10.1111/gcb.13705
Baret, Frédéric, et al. *Remote sensing of environment* (2013): https://doi.org/10.1016/j.rse.2012.12.027
Bogena, H. R., et al. *Vadose Zone Journal* (2018): https://doi.org/10.2136/vzj2018.03.0055
Camacho, Fernando, et al. *Remote Sensing of Environment* (2013): https://doi.org/10.1016/j.rse.2013.02.030
Jager, H. J., et al. *Journal of Applied Botany* 77.5/6 (2003): 117-127.
Knorr, W., et al. *Journal of Geophysical Research: Biogeosciences* (2010): https://doi.org/10.1029/2009JG001119
Post, Hanna, et al. *Biogeosciences* (2018): https://doi.org/10.5194/bg-15-187-2018
Rauthe, Monika, et al. *Meteorologische Zeitschrift* (2013): https://doi.org/10.1127/0941-2948/2013/0436
Schulz, Jan-Peter, Gerd Vogel, and Bodo Ahrens. *COSMO Newsletter* 15 (2015): http://www.cosmo-model.org/

JUSTUS-LIEBIG-UNIVERSITÄT GIESSEN

CLM Community

Annual Cycle of LAI

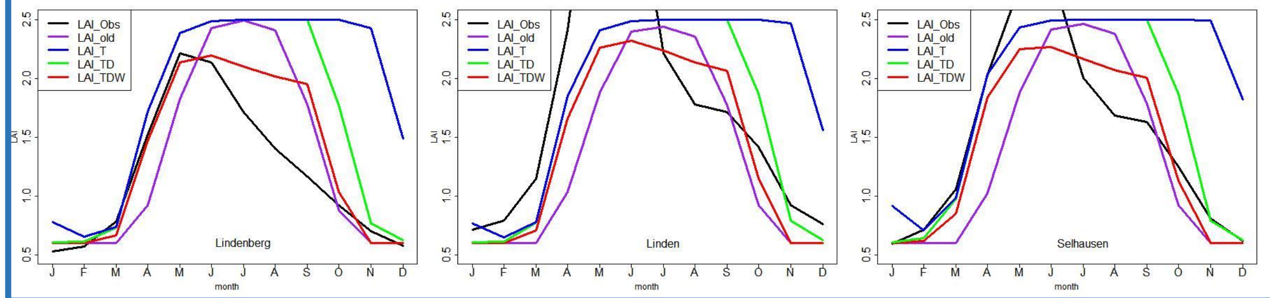

Fig.1: Mean (1999-2015) annual cycle of LAI. Results with the standard phenology (_old, purple), only the dependence on temperature (_T, blue), the dependence on day length added (_TD, green), the fully implemented new phenology (_TDW, red), and satellite observations (_Obs, black) are shown at Lindenberg, Linden, and Selhausen.

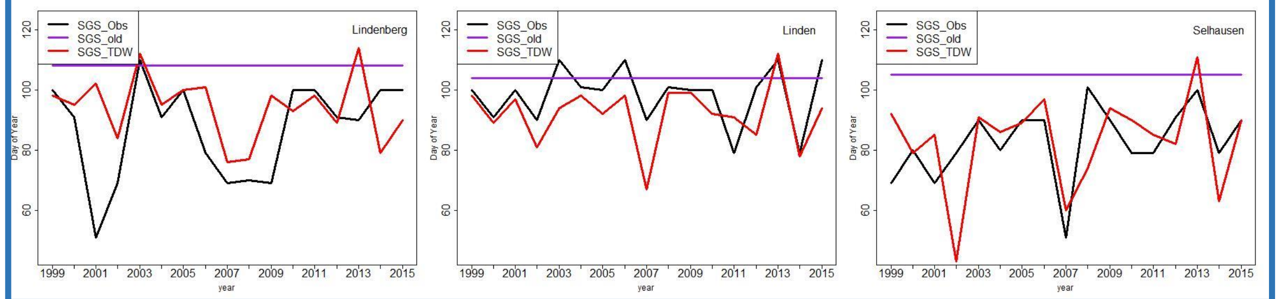

Fig.2: Start of the growing season (SGS) in number of days at each year from 1999 to 2015 and each domain (Lindenberg, Linden, and Selhausen) for satellite observations (_Obs, black), the standard phenology simulations (_old, purple), and the new phenology simulations (_TDW, red).

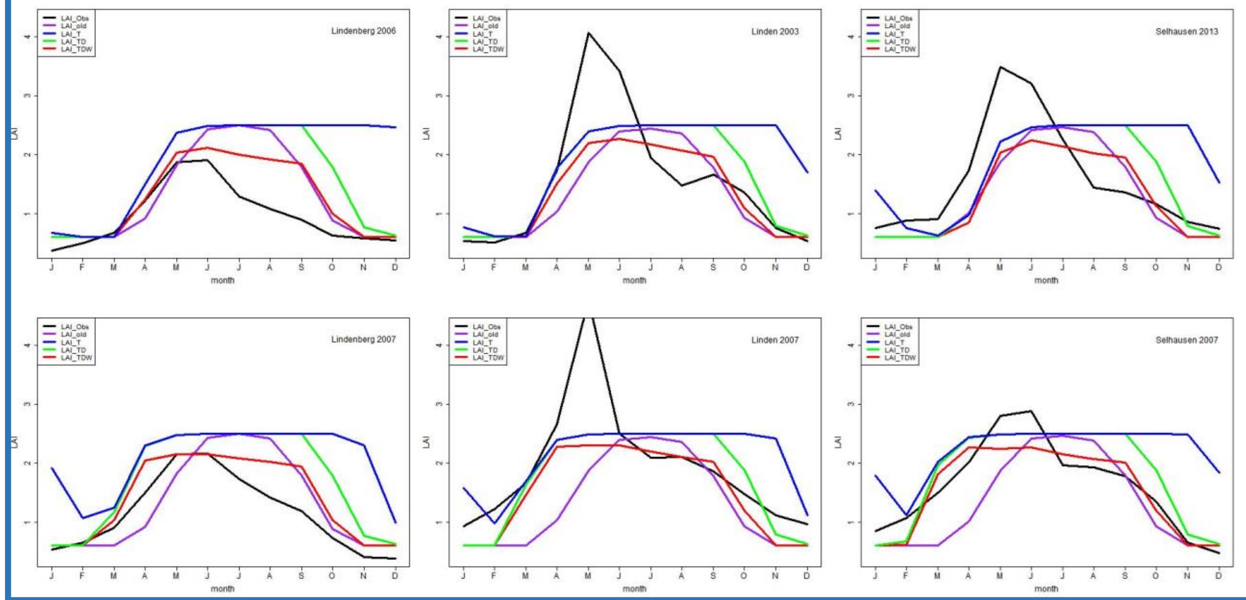

Fig.3: Annual cycle of LAI for exceptional dry years (summer) 2006 (Lindenberg), 2003 (Linden), and 2013 (Selhausen) (upper part), and for the exceptional warm year (winter/spring) 2006 (Lindenberg, Linden, Selhausen) (lower part). Results with the standard phenology (_old, purple), only the dependence on temperature (_T, blue), the dependence on day length added (_TD, green), the fully implemented new phenology (_TDW, red), and satellite observations (_Obs, black) are shown.

Results I

- The mean annual cycle of LAI improved regarding start, peak, and end of the growing season (Fig. 1)
- The interannual variability of the start of the growing season is comparable to the observations (Fig. 2)
- The representation of extreme years with an earlier start and lower summer values of LAI also improved (Fig. 3)

JUSTUS-LIEBIG-UNIVERSITÄT GIESSEN

Influences of Phenology on the Atmosphere

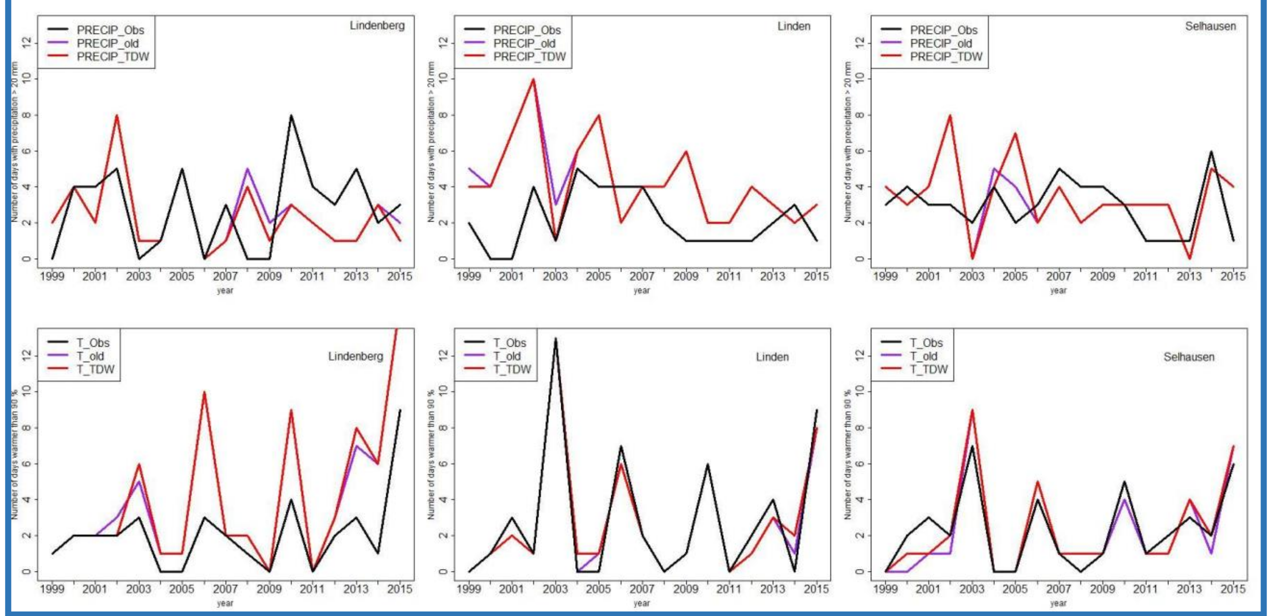

Fig.4: Heavy precipitation events with more than 20 mm per day (top) and very warm days within the 90 th Percentile of the observed maximum temperatures (bottom) in each year of the period 1999 to 2015 at Lindenberg, Linden and Selhausen for the HYRAS observations (_Obs, black), the standard phenology simulations (_old, purple), and the new phenology simulations (_TDW, red).

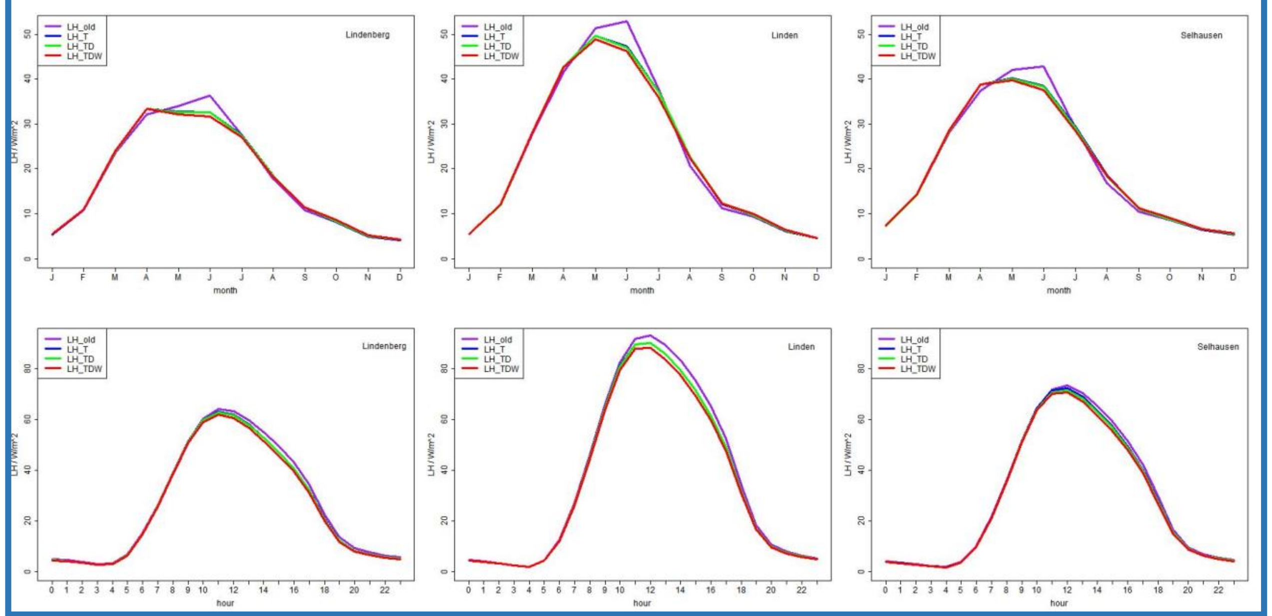

Fig.5: Mean (1999-2015) annual latent heat flux (top) and mean (1999-2015) daily latent heat flux during summer JJA (bottom) at Lindenberg, Linden and Selhausen for the simulations with the standard phenology (_old, purple), only the dependence on temperature (_T, blue), the dependence on day length added (_TD, green), and the fully implemented new phenology (_TDW, red).

Results II

- The total number of days with heavy precipitation is closer to the observations in more years with the new phenology (Fig. 4, top)
- The average number of extreme warm days is closer to the observations with the new phenology (Fig. 4, bottom)
- The latent heat flux in summer is with the new phenology reduced due to less available water (Fig. 5, top)
- In summer the mean daily latent heat flux is reduced due to less available water during the day (Fig. 5, bottom)